Photophysics of Ochratoxin A in Aqueous Solution

Dörte Steinbrück, Claudia Rasch, and Michael U. Kumke

Institute of Chemistry, University of Potsdam,
Karl-Liebknecht-Straße 24 – 25, 14476 Potsdam, Germany

Reprint requests to Michael U. Kumke. E-mail: kumke@chem.uni-potsdam.de

The photophysics of Ochratoxin A (OTA) in aqueous solution strongly depends on the pH. Due to its molecular structure OTA is prone to an excited state proton transfer reaction, which rules the photophysical properties. Based on results of absorption and fluorescence measurements the rate constants of the proton transfer reactions (forward and back reaction) were determined and subsequently, the $pK_a^\star$ value was calculated. Based on the results, optimized experimental conditions for the analysis can be determined *e. g.*, solvent conditions (HPLC chromatography) or excitation and emission wavelength (fluorescence spectroscopy).

Key words: Ochratoxin A, Proton Transfer, Excited State Kinetics, Photophysics, Fluorescence Detection

Introduction

Mycotoxins are toxic fungal metabolites that may contaminate primary food products such as nuts, cereals and fruits. One of the predominant mycotoxins in central and eastern Europe is ochratoxin A (OTA, see Fig. 1) produced by several storage fungis such as *Aspergillus* and *Penicillium* species [1]. OTA is cytotoxic, carcinogenic, mutagenic, and immunosuppressive. Because of the potential health risks for humans and animals a fast-growing need for reliable, sensitive, and selective analytical methods exists. Especially methods based on fluorescence spectroscopy are highly attractive because of their outstanding sensitivity and selectivity. Fluorescence spectroscopy is already widely used in combination with separation techniques like HPLC as a powerful analytical technique in biomedical sciences and environmental monitoring applications [2 – 5]. As is true for other analytical methods fluorescence has its limitations, some of which originate from interferences arising from the chemistry of the sample.

In order to utilize a fluorescence technique for the analysis of OTA in food and feed stuff as well as for basic research on the fungal metabolism of OTA (*e. g.*, release of OTA or distribution of OTA on grains), the photochemistry and photophysics of OTA need to be elucidated in detail, especially the influence of solvent parameters such as polarity, ionic strength, and pH.
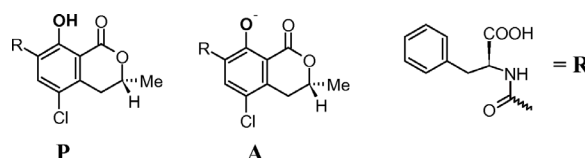

Fig. 1. Chemical structure of OTA.

Recently, basic photophysical data, namely absorption and fluorescence spectra, have been reported [6 – 11].

It has been shown that the fluorescence parameters (such as the fluorescence maximum) of OTA are strongly dependent on the pH of the solution and in general on the solvent used. It was concluded that the phenolic group undergoes an excited state proton transfer (ESIPT) reaction [12, 13]. Depending on the solvent used an inter- as well as an intramolecular proton transfer reaction can be operative.

Such excited-state proton exchange reactions are well established for molecules which contain electron withdrawing or donating groups directly attached to an aromatic molecule. In case of the electron donating OH-group the electron density of the O-H-bond is decreased and subsequently the acidity of this group can be dramatically increased in the electronically excited state [14]. For molecules such as 2-naphthol the acidity of the -OH-group is increased by almost seven(!) orders of magnitude (pK_a of 9 in the ground state compared to $pK_a^\star$ of about 2 in the excited state [15]). It is of utmost primary analytical importance that alteration

of acidity and basicity of (analyte) molecules in their electronically excited states are taken into account in order to minimize serious limitations upon sensitivity, selectivity, and accuracy of analytical methods based on fluorescence.

In the present study the fluorescence properties of OTA as a function of pH were investigated in detail. Absorption and fluorescence spectra as well as fluorescence quantum efficiency and fluorescence decay times were determined in the pH range of $1 \leq$ pH ≤ 11. Especially the pH dependence of the fluorescence decay was investigated and evaluated in order to determine the p$K_a^\star$ from the rate constants of the (de)protonation reaction in the electronically excited state of OTA.

Experimental Section

OTA was purchased from Sigma-Aldrich ($\geq$ 98 % purity, produced by *Aspergillus Ochraceus*) and used as received. The sample solutions were prepared in Millipore water. Because it is known that OTA slowly decomposes in solution, samples were freshly prepared prior to the measurements [13]. For the pH adjustment of the solutions HCl and NaOH (both purchased from Carl Roth, Karlsruhe) were added. The absorption measurements were carried out using a Lambda 750 UV/Vis Spectrometer (Perkin Elmer). The steady-state fluorescence measurements were performed on a FlouroMax3-P spectrometer (Jobin Yvon). An FLS920 Spectrofluorometer (Edingburgh Instruments) was employed in the time-resolved fluorescence measurements and operated in the time-correlated single photon counting (TCSPC) mode. For excitation pulsed light emitting diodes ($\lambda_{ex} =$ 320 nm and 375 nm, respectively, Edingburgh Instruments) or a titan-saphire laser were used. The titan-saphire laser was operated at $\lambda =$ 720 nm, and the output wavelength was doubled using second harmonic generation ($\lambda_{ex} =$ 360 nm, Tsunami 3960, Spectra Physics). The fluorescence quantum efficiencies were determined using an integrating sphere set-up (PL Quantum Yield Measurement System C9920-02, Hamamatsu).

Data analysis

The fluorescence decays were analyzed using the commercial software package FLUORESCENCE ANALYSIS SOFTWARE TECHNOLOGY (FAST, Edinburgh Instruments).

Briefly, the experimental data were evaluated using Eq. 1.

$$I(t) = A + a_1 e^{-\gamma_1 t} + a_2 e^{-\gamma_2 t} \qquad (1)$$

According to the kinetic scheme commonly applied in the analysis of excited state proton transfer reactions (see Fig. 2),
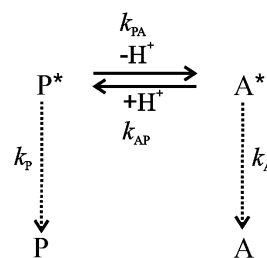

Fig. 2. Scheme of an excited state proton transfer reaction. The $\star$ indicates that the molecule is in an electronically excited state.

the time constants $\gamma_{1,2}$ are functions of the rate constants corresponding to the different radiative and non-radiative deactivation processes of the protonated (P) and deprotonated (A) molecule as well as the pH of the solution [16, 17].

$$\gamma_{1,2} = \frac{(X+Y) \pm \sqrt{(Y-X)^2 + 4k_{PA} k_{AP}[H^+]}}{2} \qquad (2)$$

with $X = k_{PA} + k_P$ and $Y = k_{AP}[H^+] + k_A$.

The rate constants k_P and k_A can be determined from measurements at low and high pH, respectively.

The parameters $\gamma_{1,2}$ are dependent on the pH:

$$\gamma_1 + \gamma_2 = k_P + k_{PA} + k_A + k_{AP}[H^+], \qquad (3)$$

$$\gamma_1 \cdot \gamma_2 = XY - k_{PA} k_{AP}[H^+], \qquad (4)$$

From the evaluation of $\gamma_1 + \gamma_2$ and $\gamma_1 \cdot \gamma_2$ as a function of pH the rate constants k_{PA} and k_{AP} can be obtained (see Eqs. 3 and 4) and subsequently $K_a^\star$ can be calculated according to Eq. 5.

$$\frac{k_{PA}}{k_{AP}} = K_a^\star \qquad (5)$$

Results and Discussion

Absorption and steady-state fluorescence

In Fig. 3 the absorption and the fluorescence emission as well as the fluorescence excitation spectra at different pH are shown. At pH < 4.5 the longest wavelength absorption maximum is located at $\lambda_{abs,max} =$ 333 nm. Upon increasing the pH the absorption of OTA is red-shifted. At pH > 4.5 a second maximum starts to evolve at $\lambda_{abs,max} =$ 380 nm. At high pH only the latter absorption maximum is found.

In contrast to the absorption, the fluorescence emission is shifted toward shorter wavelength with increasing pH. At pH < 1 the fluorescence maximum is located at $\lambda_{em,max} =$ 470 nm and is blue-shifted with increasing pH to $\lambda_{em,max} =$ 440 nm. The very

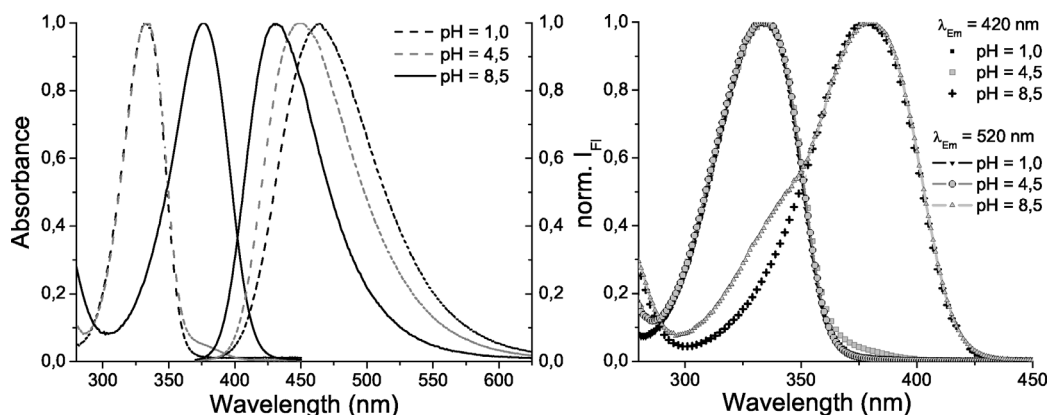Fig. 3. Absorption and emission spectra (λ_{ex} = 333 nm) of OTA at different pH values (left). Excitation spectra (different λ_{em}) of OTA in dependence on pH value (right).

large Stokes shift of about 8700 cm^{-1} is decreased to about 3500 cm^{-1} at higher pH as has been reported before [6]. The observed large Stokes shifts already indicate that due to light absorption a significant change of the charge distribution in the molecule is induced.

The fluorescence quantum efficiencies were determined for the fully protonated and the fully deprotonated form of OTA to be relatively similar. A fluorescence quantum efficiency ϕ at pH = 1 (λ_{ex} = 333 nm) and pH = 9 (λ_{ex} = 380 nm) of ϕ = 42 % and ϕ = 53 %, respectively, were measured.

From the fluorescence excitation spectra the presence of an excited state reaction can readily be concluded. For pH < 4.5 – independent on the emission wavelength set (λ_{em} = 420 nm or λ_{em} = 520 nm, see Fig. 3, right) – only one absorption maximum at λ_{ex} = 330 nm is observed. At high pH a second maximum at λ_{ex} = 380 nm is found, which corresponds well to the observed trends in the absorption spectra. At low pH only one (protonated) species is present in the electronic ground state, however, after excitation a second species is formed. The spectroscopic properties correspond to the species that is found in solution at high pH.

The pH-dependence of the relative absorption and fluorescence intensity is shown in Fig. 4. Absorption and fluorescence data show different inflection points. From the molecular structure of OTA two groups sensitive to pH alterations can be identified: the carboxylic group and the hydroxy group of the isochroman-1-one moiety. The acid constants given as the pK_a values are around 4 for the carboxylic group and around 7 for the hydroxy group [18]. The latter is compared to

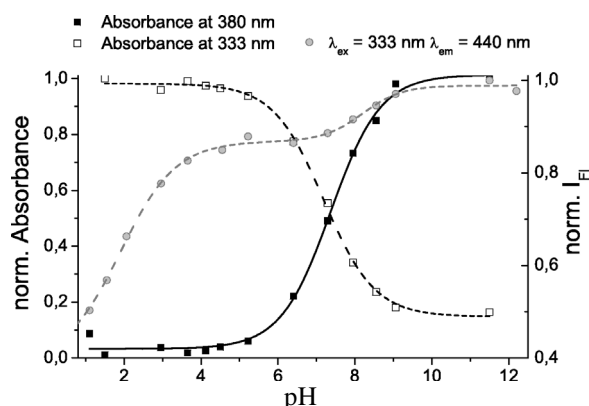Fig. 4. Dependence of the absorption at λ = 333 nm and λ = 380 nm as well as of the fluorescence intensity at λ_{em} = 440 nm (λ_{ex} = 333 nm) on the pH.

other phenolic compounds (or to ochratoxin B) lowered due to the presence of the chlorine atom in para position (see Fig. 1). From the absorption data an inflection point around pH = 7 is found, which is in very good agreement with the pK_a of the hydroxy group of the isochroman-1-one moiety. On the other hand, the pH-dependence of the fluorescence intensity exhibits an inflection point at a significantly lower pH ($\approx$ 2) and a (smaller) second one around pH = 7. The observed alterations in the absorption and fluorescence spectra of OTA can be attributed to the (de)protonation of the hydroxy group because i) the carboxylic group is not directly attached to the aromatic system and consequently (de)protonation of this group should have – if any – only a very minor effect on the photophysical properties and ii) the *o*-methyl ether of OTA, which has no potential acidic phenolic proton, shows
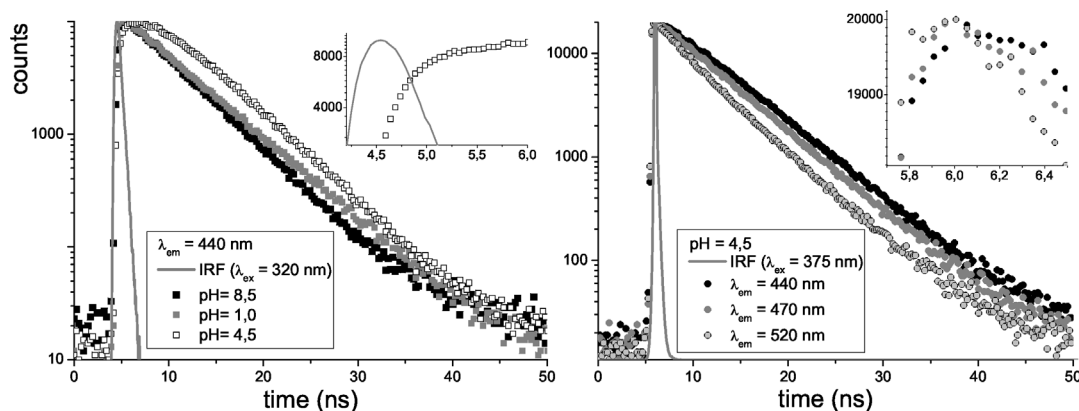
Fig. 5. Fluorescence decay curves of OTA at different pH (λ_{ex} = 320 nm, λ_{em} = 440 nm) (left). Fluorescence decay curves of OTA at different λ_{em} and constant pH (right).

fluorescence spectra very similar to OTA at high pH. While in the absorption measurements the electronic ground state of the molecule is probed, the fluorescence data yield information on the electronically excited state, and consequently the low inflection point indicates that the p$K_a^\star$ of OTA is greatly different compared to the ground state because of an excited state proton transfer reaction. This has been suggested before [6].

For the determination of the p$K_a^\star$ value the steady-state fluorescence and absorption spectra were evaluated according to the well-known Förster cycle. A p$K_a^\star$ of about 5 was determined. However, because of the extremely large Stokes shift the exact determination of the 0-0-transitions of the protonated (P) and deprotonated (A) form is very difficult, and the analysis is consequently prone to large errors [14]. In such cases the determination of p$K_a^\star$ is best done from time-resolved fluorescence measurements at different pH.

Fluorescence decay

In order to further elucidate the proton transfer reaction occurring in the electronically excited state, time-resolved fluorescence measurements were performed in the pH-range of $0.4 < \text{pH} < 7$ with λ_{ex} = 320 nm and λ_{em} = 440 nm. The excitation wavelength corresponded to the absorption maximum of protonated OTA (form P), while the fluorescence detection was set to the emission maximum of the deprotonated species (form A) which is formed in the excited state (or at high pH). To determine the fluorescence decay times of P and A, additional measurements were carried out

Table 1. Basic photophysical parameters of OTA.

	$\lambda_{ab,max}$ (nm)	$\lambda_{em,max}$ (nm)	τ (ns)	ϕ (%)
OTA P	330	470	5.9	42
OTA A	380	440	5.1	53

at pH < 1 (λ_{ex} = 320 nm and λ_{em} = 520 nm) and at pH = 9 (λ_{ex} = 375 nm and λ_{em} = 440 nm), respectively. The fluorescence decays at pH < 1 and at pH > 7 followed a first order decay law and could be fitted monoexponentially (see Fig. 5). At pH < 1 a fluorescence decay time τ_P = 5.9 ns and at pH > 7 a fluorescence decay time τ_A = 5.1 ns was determined.

In the intermediate pH-range $1 < \text{pH} < 7$ complex fluorescence decays were observed (see Fig. 5). At short times after the excitation laser pulse a clear increase of the fluorescence intensity (rise) was found, which indicates the formation of a new species (*e. g.*, due to deprotonation) in the electronically excited state (see inset Fig. 5, left) [17]. The observation of this rise was dependent on the fluorescence emission wavelength (see Fig. 5, right). It was clearly observed at the short wavelength range of the fluorescence spectrum of OTA, while at longer emission wavelengths (λ_{em} > 470 nm) such rise was not found. This is due to the fact that the fluorescence spectra of the P and A form of OTA strongly overlap in this spectral region. From the data analysis using Eq. (1) $a_{1,2}$ as well as $\gamma_{1,2}$ were obtained. In agreement with the model of excited state reactions, in the analysis one of the amplitudes was found to be negative. In Fig. 6 the pH-dependence of $a_{1,2}$ and $\gamma_{1,2}$ is shown. At $1 < \text{pH} < 4$ the largest changes in the amplitudes $a_{1,2}$ and the decay parameters $\gamma_{1,2}$ were observed.
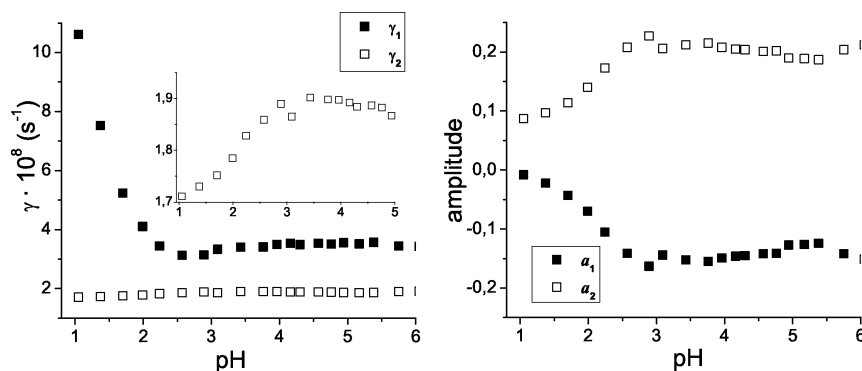
Fig. 6. pH-Dependent changes of the fluorescence decay parameters $\gamma_{1,2}$ (left) and the corresponding amplitude $a_{1,2}$ (right) for $\lambda_{\text{ex}} = 320$ nm and $\lambda_{\text{em}} = 440$ nm, respectively.
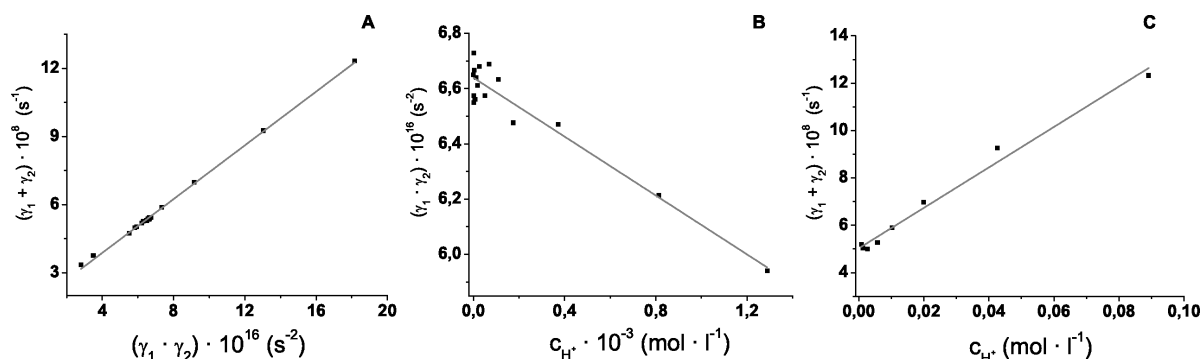

Fig. 7. Determination of the rate constants ($\lambda_{\text{ex}} = 320$ nm; $\lambda_{\text{em}} = 440$ nm). A: $k_{\text{P}} = 1.7 \cdot 10^8$ s^{-1}; B: $k_{\text{PA}} = 5.4 \cdot 10^8$ s^{-1}; C: $k_{\text{AP}} = 9.8 \cdot 10^9$ l mol^{-1} s^{-1}.

In order to extract the rate constants k_{PA} and k_{AP} of the excited state reaction (see Fig. 2), $\gamma_{1,2}$ values were evaluated according to Eqs. 2 to 4 for the intermediate pH range. As a control also k_{P} (= $\frac{1}{\tau_{\text{P}}}$) was calculated (see Fig. 2). From the data evaluation $k_{\text{P}} = 1.7 \cdot 10^8$ s^{-1} was determined, which corresponds to $\tau_{\text{P}} = 5.9$ ns and is in excellent agreement with the decay time found at pH < 1. The rate constants of (de)protonation were determined to $k_{\text{PA}} = 5.4 \cdot 10^8$ s^{-1} and $k_{\text{AP}} = 9.8 \cdot 10^9$ l mol^{-1} s^{-1}, respectively (Fig. 7). According to Eq. 5 the p$K_a^\star$ value was calculated to be 1.5 ± 0.4.

Conclusions

At low pH (< 5) only the absorption spectra of the protonated form (P) of OTA are observed, while in the fluorescence spectra already at pH > 1 both forms (P and A) are found, which is due to the presence of a photoinduced proton transfer. The large Stokes shift indicates that upon excitation a significant charge redistribution occurs in the molecule. Based on the ex-

perimental data this can be attributed to the deprotonation of the hydroxy group of the isochroman-1-one moiety. This is in line with the general trend found for electron donor groups such as hydroxy groups directly attached to an aromatic system. Due to the electronic excitation, the O-H bond strength is decreased, and subsequently the hydroxy group becomes more acidic (p$K_a^\star$ < pK_a) [14]. A showcase for such systems is 2-naphthol [15]. For the methoxy compound of OTA no such effects were observed, since an excited state proton transfer is not possible there. Moreover, in the spectra of OTA in DMF, which can act as a strong base, only the A form was observed. These findings further strongly support the assignment of the hydroxy group of the isochroman-1-one moiety as the source for the observed photophysical effects.

Based on the time-resolved fluorescence data analysis the acidity constant in the electronically excited state p$K_a^\star$ was determined to 1.5 ± 0.4, which corresponds to an increase in the acidity of the hydroxy group of approximately five orders of magnitude compared to the ground state (p$K_a \approx 7$).

Recently, an intramolecular proton transfer to the adjacent keto group was suggested to be operative [6]. The rate for such an intramolecular proton transfer (keto-enol tautomerism) is expected to be very high (ps time scale) and would not be resolved in the time-resolved fluorescence measurements performed. Consequently, the observation of the fluorescence rise within the first nanoseconds after excitation is a strong indication that the proton transfer reaction is intermolecular, and this is supported by the rate constants determined. Because the fluorescence spectra of the P and A form strongly overlap, this rise can only be unambiguously observed at the blue edge of the fluorescence spectrum at medium pH levels. It is very attractive to propose solvent molecules, like water, as the most probable proton acceptors. The determined rate constants for (de)protonation k_{PA} and k_{AP}, respectively, are well within the range commonly observed for solvent-assisted intermolecular proton transfer reactions, *e. g.* for 2-naphthol in water [15].

Recognizing that an excited-state proton exchange process does occur during the lifetime of the electronically excited state of OTA, it is necessary to consider that this process can interfere with the fluorometric analysis in case the pH of the test solution (sample) lies in the range where excited-state prototropism occurs (*e. g.*, in case of water as solvent) or when a solvent with good proton accepting properties is used. With the determination of the p$K^\star$ value it is now possible to adjust the experimental conditions accordingly and thus, to eliminate the influence of the excited-state prototropic reactivity minimizing the effect as a potential analytical interference. For OTA it has to be recognized that only at pH > 7 the excited-state proton transfer is not interfering, because in that case the major portion of OTA is in its A form. However, at higher pH OTA is not (photo)stable (hydrolysis of the lactone ring) [19, 20]. Consequently, this will limit the analysis at high pH.

These spectroscopy results can be used in the development of an improved analysis and of *in situ* as well as in-line sensing schemes for OTA, *e. g.*, along the food chain. As a major implication, a two-wavelength excitation/detection scheme with the two $\lambda_{ex}/\lambda_{em}$ pairs 330 nm / > 470 nm and 380 nm / 440 nm is suggested. Work is in progress to use such a fluorescence set-up in combination with diffuse reflectance spectroscopy (operated in the NIR spectral range) for *in situ* monitoring of OTA contamination of grains in the field and in storage facilities.

[1] J. W. Bennett, M. Klich, *Clinical Microbiology Reviews* **2003**, *16*, 497 – 516.

[2] C. M. Maragos, *J. o. Toxicology. Toxin Reviews* **2004**, *23*, 317 – 344.

[3] Y. Kostov, G. Rao, *Rev. Sci. Instrum.* **2000**, *71*, 4361 – 4373.

[4] S. Nakai, Y. Horimoto, *Encyclopedia of Analytical Chemistry* **2006**, *9*, 1 – 12.

[5] L. Monaci, *Analytical and Bioanalytical Chemistry* **2004**, *378*, 96 – 103.

[6] Y. V. Il'ichev, J. L. Perry, R. A. Manderville, C. F. Chignell, J. D. Simon, *Journal of Physical Chemistry B* **2001**, *105*, 11369 – 11376.

[7] A. E. Pohland, P. L. Schuller, *Pure and Applied Chemistry* **1982**, *54*, 2219 – 2284.

[8] F. S. Chu, *Life Sciences* **1972**, *11*, 503 – 508.

[9] R. Krska, *Analytical and Bioanalytical Chemistry* **2007**, *387*, 145 – 148.

[10] R. Verrone, L. Catucci, P. Cosma, P. Fini, *Journal of Inclusion Phenomena and Macrocyclic Chemistry* **2007**, *57*, 475 – 479.

[11] P. Bayman, *Mycopathologia* **2006**, *162*, 215 – 223.

[12] C. Frennette, *Anal. Chim. Acta* **2008**, *617*, 153 – 161.

[13] M. E. Brow, *Photochemistry and Photobiology* **2002**, *76*, 649 – 656.

[14] S. G. Schulman, *Modern Fluorescence Spectroscopy Part 1*, Heyden, **1976**.

[15] R. Boyer, A. M. Halpern, *Journal of Chemical Education* **1985**, *62*, 630 – 632.

[16] B. Valeur, *Molecular Fluorescence – Principles and Applications*, Wiley-VCH, Vol. 1, **2002**.

[17] J. B. Birks, *Photophysics of Aromatic Molecules*, Wiley-Interscience, London, **1970**, pp. 301 – 308.

[18] J. Dai, *Accounts of Chemical Research* **2004**, *37*, 874 – 881.

[19] H. Xiao, S. Madhyastha, R. R Marquardt, S. Li, J. K. Vodela, A. A. Frohlich, B. W. Kemppainen, *Toxicology and Applied Pharmacology* **1996**, *137*, 182 – 192.

[20] M. A. Stander, *Chem. Res. Toxicol.* **2001**, *14*, 302 – 304.